

UNCLASSIFIED

AD NUMBER
AD902605
NEW LIMITATION CHANGE
TO Approved for public release, distribution unlimited
FROM Distribution authorized to U.S. Gov't. agencies only; Administrative/Operational Use; 20 Jul 1972. Other requests shall be referred to Naval Air Systems Command, Washington, DC 20360.
AUTHORITY
NRL ltr, 27 Jun 1983

THIS PAGE IS UNCLASSIFIED

AD 902605

AUTHORITY: NRL / Fr, 27 Jun 83



CONTENTS

Abstract	ii
Authorization	ii
INTRODUCTION	1
EFFECT OF PLATFORM MOTION ON MTI PERFORMANCE	1
DESCRIPTION OF DPCA	4
EFFECT OF DPCA ON MTI PERFORMANCE	7
CONCLUSIONS	8
REFERENCES	9
APPENDIX A—Derivation of Phase Advance Due to Platform Motion	10
APPENDIX B—Derivation of the Transfer Function of an MTI with DPCA	12
APPENDIX C—Derivation of the MTI Improvement Factor with DPCA	15
APPENDIX D—Evaluation of DPCA with $\sin x/x$ Antenna Pattern	21

ABSTRACT

Coherent signal processing in an airborne radar is highly dependent upon methods used to compensate for platform (e.g., airplane) motion. Platform motion causes returns to have doppler shifts which vary with the angle between the velocity vector of the platform and that of the target or scatterer. Because of the finite antenna beamwidth and the finite transmitted pulse length, radar returns from many scatterers are received simultaneously from different angles. Therefore, these returns combine to give a spectrum of doppler frequencies which must be corrected.

Displaced Phase Center Antenna (DPCA) is a technique which compensates for the component of motion which is perpendicular to the axis of the beam. This report evaluates DPCA in terms of its improvement to airborne moving target indicator (MTI) performance. It is shown that MTI performance is improved significantly with DPCA. However, since DPCA does not completely compensate for this motion, MTI performance can be limited by this technique under certain conditions.

AUTHORIZATION

NRL Problem R02-29
Project A360-5333/652B/2F00-141-601

Manuscript submitted April 13, 1972.

AIRBORNE RADAR MOTION COMPENSATION TECHNIQUES— EVALUATION OF DPCA

INTRODUCTION

Motion compensation is a fundamental need for a search radar system operated from a moving platform. The application of digital processing techniques to radar signals has made it practical to coherently process many radar returns using moving target indicators (MTI) with multiple-stage cancellers and coherent integration (narrow-band doppler filtering). The resulting theoretical clutter rejection capability increases the detection of moving targets in clutter to such a point that other system limitations become the dominant concern.

The full capability of this coherent processing can be realized only through the use of motion compensation to remove the doppler contributions caused by platform motion. With existing motion compensation techniques, the radar system may then be limited by other factors, such as system stability or on-aircraft antenna sidelobes. As these other system limitations are improved, it becomes necessary to reconsider the motion compensation techniques to determine at what level the system is again limited by these techniques.

It is in this context that Displaced Phase Center Antenna (DPCA) is considered. Time Averaged Clutter Coherent Airborne Radar (TACCAR), which corrects for the platform velocity component parallel to the axis of the antenna beam pattern, and DPCA, which corrects for the perpendicular component of platform velocity, make up the motion compensation techniques which are being applied to present early-warning radar systems. An evaluation of TACCAR is presented in Ref. 1.

The success of a motion compensation technique must be evaluated in terms of its improvement to the signal processing in the radar receiver. Since many airborne radar systems now (and in the foreseeable future) involve MTI processing, the improvement in MTI gain will be used to measure the performance of DPCA.

EFFECT OF PLATFORM MOTION ON MTI PERFORMANCE

The objective of most coherent radar processors is to discriminate between the returns from moving and fixed targets. For some radar applications, the returns from fixed objects are of interest. However, for the MTI radar, these returns are considered as "clutter" and should be rejected. The rejection decision (or filtering) is based on the doppler shift of the frequency of the returns. If the radar itself is on a moving platform, the returns from fixed objects will also have doppler shifts. This doppler shift of the returns from fixed objects must be corrected to provide good MTI performance.

In Ref. 1, the doppler shift f_d of the return from a scatterer caused by platform motion is given by

$$f_d = -2 \frac{v_p}{\lambda} \cos \phi_s \cos \theta_s \quad (1)$$

where

- v_p = aircraft (platform) velocity vector,
- λ = transmitted wavelength
- ϕ_s = vertical angle between v_p and the direction vector to the scatterer, and
- θ_s = horizontal angle between v_p and the direction vector to the scatterer.

When the axis of the antenna pattern is pointing in a direction given by the direction angles θ_a, ϕ_a relative to v_p , and the scatterer is in the direction θ, ϕ with respect to the axis of the antenna pattern, then

$$\theta_s = \theta_a + \theta.$$

So

$$\begin{aligned} f_d &= -2 \frac{v_p}{\lambda} \cos \phi_s \cos(\theta_a + \theta) \\ &= -2 \frac{v_p}{\lambda} \cos \phi_s (\cos \theta_a \cos \theta - \sin \theta_a \sin \theta). \end{aligned}$$

Averaging f_d over a symmetrical antenna pattern gives

$$\bar{f}_d = -2 \frac{v_p}{\lambda} \cos \phi_s \cos \theta_a. \quad (2)$$

From Ref. 1, the purpose of TACCAR is to estimate \bar{f}_d and remove this component of doppler shift. When this component is removed, the remaining doppler shift is

$$f'_d = -2 \frac{v_p}{\lambda} \cos \phi_s [\cos \theta_a (\cos \theta - 1) - \sin \theta_a \sin \theta]. \quad (3)$$

By assuming a highly directive antenna pattern so that the range of interest for θ is small, the small-angle approximation for Eq. (3) leads to

$$f'_d \approx 2 \frac{v_y}{\lambda} \theta$$

where

$$v_y = v_p \cos \phi_s \sin \theta_a.$$

This relation shows that after the TACCAR correction, there remains a doppler shift that is approximately proportional to the angle θ of the scatterer with respect to the axis of the antenna pattern. Therefore, for homogeneous clutter, a platform-motion clutter spectrum results which is weighted by the two-way pattern of the antenna. In Ref. 2, it is shown that this spectrum can be approximated by a Gaussian spectrum with a zero mean and a standard deviation given by

$$\sigma_{PM} \approx 0.6 \frac{v_y}{a} \quad (4)$$

where a is the aperture length of the antenna.

In App. A of Ref. 1 it was shown that the MTI improvement factor for a zero-mean Gaussian clutter spectrum is given by

$$I_n = \frac{2^n}{n!} \left(\frac{f_r}{2\pi\sigma_c} \right)^{2n}$$

where

- f_r = pulse repetition frequency,
- σ_c = standard deviation of the clutter spectrum, and
- n = number of delay lines in MTI processor.

Using Eq. 4, the limitation to the MTI improvement factor caused by platform motion is

$$(I_n)_{PM} = \frac{2^n}{n!} \left(\frac{1}{1.2\pi} \frac{a}{v_y T} \right)^{2n}$$

where $T = 1/f_r$ is the pulse repetition period. This equation is plotted in Fig. 1 with n as a parameter. The expression $v_y T/a$ represents the fraction of the antenna aperture that the antenna is displaced during an interpulse period. Figure 1 illustrates the limitation to the MTI improvement factor caused by platform motion.

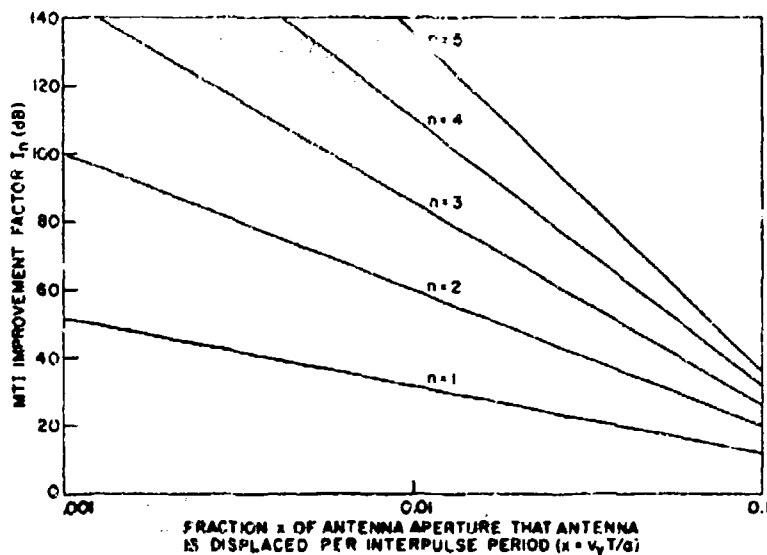


Fig. 1—Limitation of the platform motion x on the MTI improvement factor I_n for several values of the parameter n (the number of delay lines in the MTI processor)

Combining the standard deviation of the clutter spectrum due to internal clutter motion with that due to platform motion, the total standard deviation of the spectrum is

$$\sigma_T^2 = \sigma_c^2 + \sigma_{PM}^2,$$

and the total MTI improvement factor is

$$(I_n)_{\text{total}} = \frac{2^n}{n!} \left[\frac{f_r}{2\pi(\sigma_c^2 + \sigma_{PM}^2)^{1/2}} \right]^{2n}.$$

This equation gives the combined effect of internal motion and platform motion. It is plotted in Fig. 2 for a single-delay (single-canceller) MTI, in Fig. 3 for a double-delay (double-canceller) MTI, and in Fig. 4 for a triple-delay (triple-canceller) MTI. The top curves in these figures represent no platform motion. The other curves represent various degrees of platform motion. Therefore, the difference between these curves indicates the loss of MTI improvement factor due to platform motion. This loss can be appreciable for most applications when the clutter bandwidth σ_c is small.

DESCRIPTION OF DPCA

Detailed descriptions of DPCA are found in Refs. 2-4. DPCA corrects for the component of platform motion parallel to the plane of the antenna aperture by physically or electronically displacing the phase center of the antenna in the opposite direction. To see how this is accomplished, it is convenient to consider the effect of the doppler shift on the interpulse phase advance of returns. The doppler shift given by Eq. (3) can be integrated over one interpulse period to get this phase advance. Integrating f'_d , the phase advance η is

$$\eta = \int_0^T 2\pi f'_d dt.$$

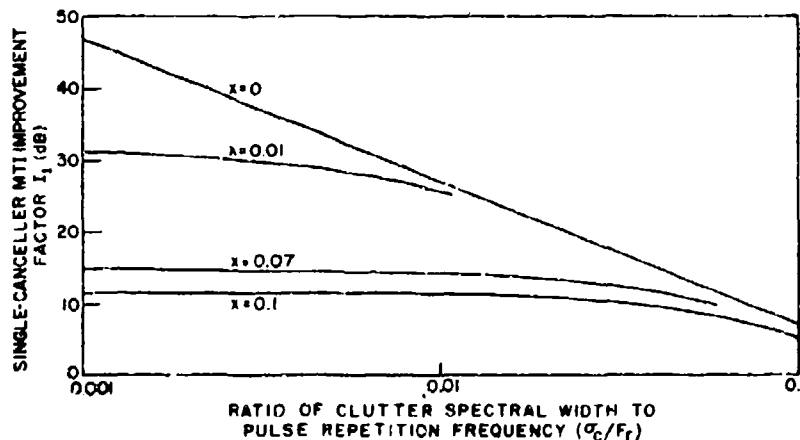


Fig. 2—Effect of platform motion of the single-canceller ($n = 1$) MTI improvement factor I_1 . x is the fraction of the antenna aperture that the antenna is displaced per interpulse period. The $x = 0$ curve represents no platform motion.

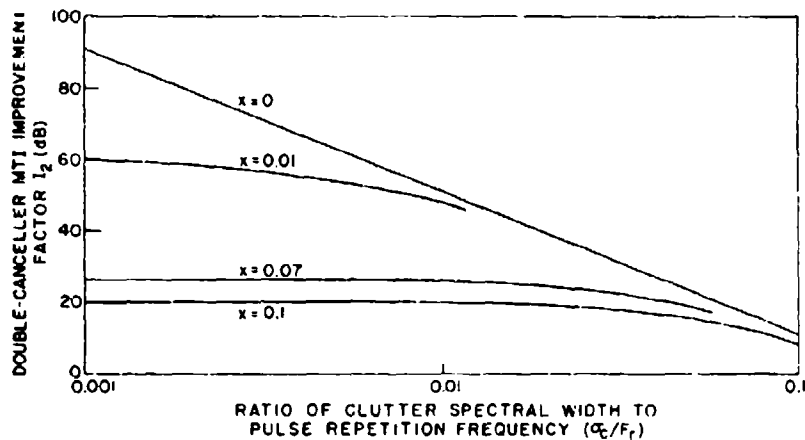


Fig. 3—Effect of platform motion on the double-canceller ($n = 2$) MTI improvement factor I_2 . x is the fraction of the antenna aperture that the antenna is displaced per interpulse period. The $x = 0$ curve represents no platform motion.

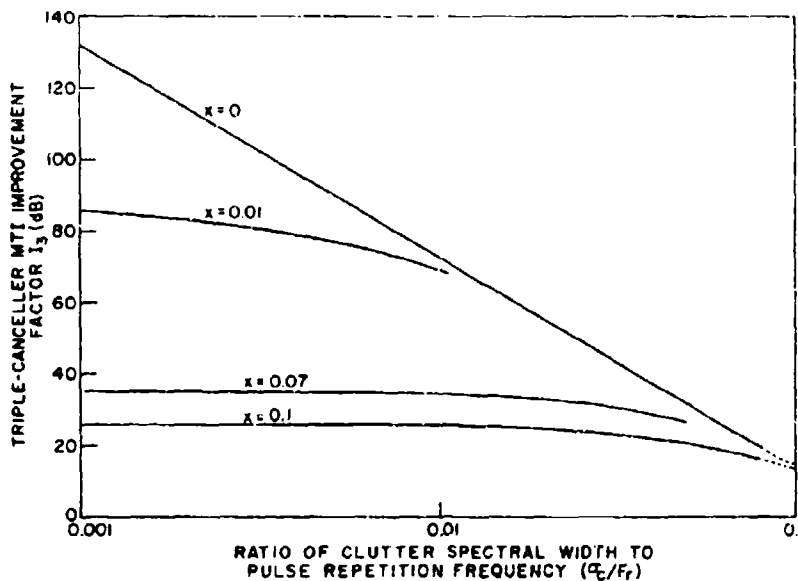


Fig. 4—Effect of platform motion on the triple-canceller ($n = 3$) MTI improvement factor I_3 . x is the fraction of the antenna aperture that the antenna is displaced per interpulse period. The $x = 0$ curve represents no platform motion.

As shown in App. A, if the product of the scan rate $\dot{\theta}$ and the interpulse period T is small, η can be approximated by

$$\eta \approx 2\pi f'_d T.$$

Also, within the main beam of a highly directive antenna pattern, Eq. (3) reduces to

$$f'_d \approx 2 \frac{v_y}{\lambda} \theta.$$

Therefore

$$\eta \approx 4\pi \frac{v_y T}{\lambda} \theta. \quad (5)$$

A point scatterer situated at an angle θ with respect to the axis of the antenna pattern has a pulse-to-pulse phase advance given by η . A vector diagram of this effect is shown in Fig. 5(a). This phase advance could be compensated with the addition of the quadrature vectors shown in Fig. 5(b). The correction vectors are given by

$$e_1 = jx_1 \tan \frac{\eta}{2}$$

and

$$e_2 = -jx_2 \tan \frac{\eta}{2}.$$

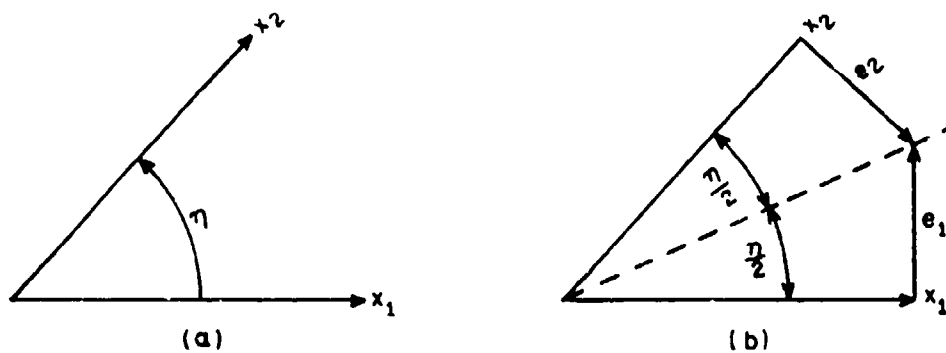


Fig. 5—Vectorial representation of (a) pulse-to-pulse advance η and (b) platform motion compensation

If the antenna pattern is $G(\theta)$, then the amplitudes x_1 and x_2 of the returns from a point source at an angle θ are modulated by the two-way pattern $G^2(\theta)$. This leads to the correction vectors

$$e_1 = jG^2(\theta) \tan \frac{\eta}{2}$$

and

$$e_2 = -jG^2(\theta) \tan \frac{\eta}{2}.$$

These vectors can be realized by transmitting the pattern $G(\theta)$ and by receiving pattern $G(\theta)$ and an additional pattern $\Delta(\theta)$ given by

$$\Delta(\theta) = jG(\theta) \tan \frac{\eta}{2}. \quad (6)$$

The returns received through the $\Delta(\theta)$ pattern are subtracted from the returns from the first pulse received through pattern $G(\theta)$ and added to the returns from the second pulse. Figure 6 is a block diagram illustrating this technique. In Ref. 2 it is shown that the pattern given by Eq. (6) can be approximated by the difference pattern of a monopulse antenna.

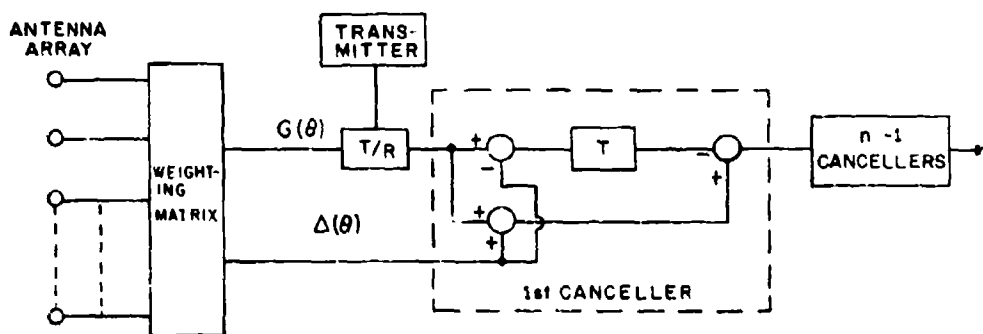


Fig. 6—Displaced Phase Center Antenna (DPCA) correction applied to the first canceller of an n -stage MTI.

EFFECT OF DPCA ON MTI PERFORMANCE

Since the antenna pattern defined by Eq. (6) generally must be approximated, the error in this pattern results in an imperfect DPCA correction and, in turn, in degraded MTI performance. This effect has been considered in Ref. 4. For the present report, it is assumed that this pattern is realized perfectly and the effect of a perfect DPCA correction on a multiple-stage MTI is evaluated.

The transfer function of an n -stage MTI with DPCA is derived in App. B. Using this result the power gain is

$$|H_{\eta}(f)|^2 = \left(1 + \tan \frac{2\eta}{2}\right) \left[2 \sin \left(\pi \frac{f-f'_d}{f_r}\right)\right]^2 \left[2 \sin \left(\pi \frac{f}{f_r}\right)\right]^{2n-2}.$$

Since η and f'_d are functions of θ , this power gain is implicitly a function of θ . The above equation shows that the null of one canceller is shifted by an amount f'_d . The other cancellers are not affected by this DPCA correction.

The MTI improvement factor associated with this transfer function is derived in App. C and given by Eq. (C5) for an n -stage MTI. Equation (C5) is evaluated further for $n = 1, 2,$ and 3 . These results are given by Eq. (C9)-(C11). An antenna pattern must be specified to use these integral equations.

These equations are evaluated in App. D using a $(\sin x)/x$ antenna pattern and integrating to the first zero crossing (main lobe). The results are plotted in Fig. D1 for a single canceller, Fig. D2 for a double canceller, and Fig. D3 for a triple canceller.

Comparing Fig. 2 with Fig. D1 it is seen that if the fraction of antenna aperture displaced per interpulse period is less than one-tenth, the MTI improvement factor for a single canceller with DPCA (Fig. D1) is essentially equal to the MTI improvement factor with zero velocity (Fig. 2). This corresponds to perfect motion compensation. For higher order cancellers this compensation is not perfect—however, there is appreciable improvement, particularly for narrow clutter spectral widths (i.e., overland). To illustrate this point, Fig. 3 and Fig. D2 are superimposed in Fig. 7, and Fig. 4 and Fig. D3 are superimposed in Fig. 8. In Fig. 7 and 8, the top curve represents the MTI improvement factor for zero velocity (or perfect compensation). The lower solid curves represent the MTI improvement factor with platform motion. The dashed curves represent the MTI improvement factor with platform motion compensated by DPCA.

CONCLUSIONS

Platform motion limits the capability of advanced airborne MTI systems attempting to obtain high cancellation ratios, as illustrated in Fig. 1. DPCA corrects only one canceller of a multiple-stage MTI. However this correction leads to significant improvement in the MTI improvement factor, especially for narrow-bandwidth clutter (i.e., overland).

Figures 7 and 8 illustrate the improvement that is achieved by DPCA. The parameter x represents the fraction of the aperture that the antenna is displaced during an interpulse period. By comparing a solid curve and a dashed curve for the same value for x , the improvement in MTI improvement factor can be determined.

Figures 7 and 8 also illustrate the additional improvement that could be achieved by a more complete compensation. The MTI improvement factor with perfect motion compensation corresponds to the MTI improvement factor with zero platform velocity. This case is represented by the curves labeled $x = 0$ (both) in Figs. 7 and 8. By comparing these curves with the dashed curves (which represent the MTI improvement factor with DPCA correction), the additional improvement that an "ideal" motion compensation

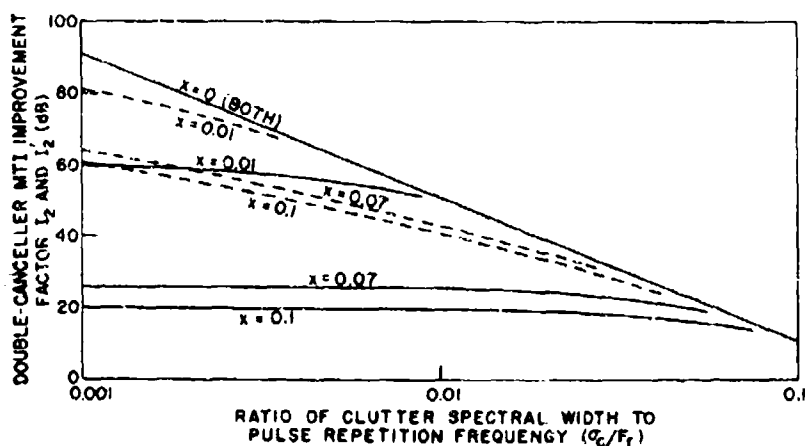


Fig. 7—Comparison of MTI improvement factor for a double-canceller ($n = 2$) with DPCA (I_2' , dashed curves) and without DPCA (I_2 , solid curves). x is the fraction of the antenna aperture that the antenna is displaced per interpulse period. The $x = 0$ curve represents no platform motion. (This figure is a superimposition of Figs. 4 and D3.)

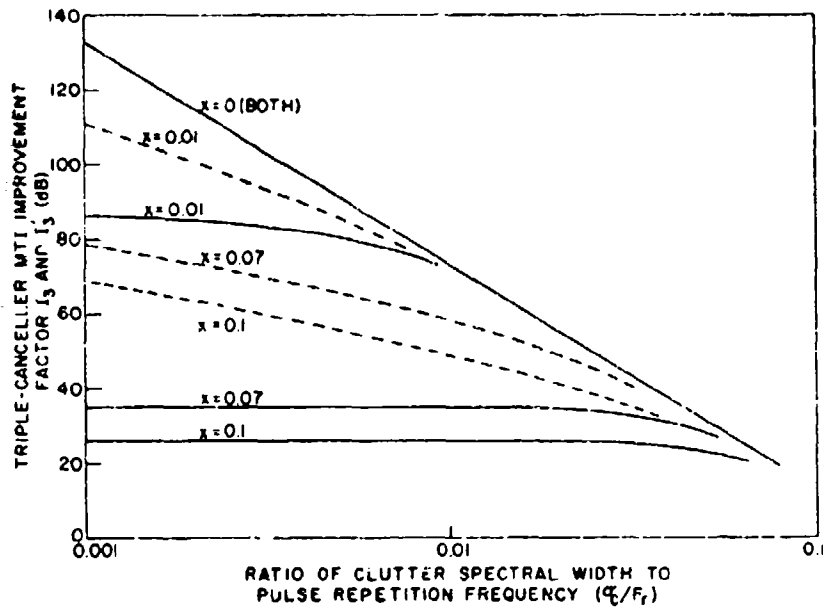


Fig. 8—Comparison of MTI improvement factor for a triple-canceller ($n = 3$) with DPCA (I_3 , dashed curves) and without DPCA (I_3 , solid curves). x is the fraction of the antenna aperture that the antenna is displaced per interpulse period. The $x = 0$ curve represents no platform motion. (This figure is a superposition of Figs. 4 and D3.)

techniques could achieve can be determined. It is seen that for narrow-band clutter (i.e., σ_c/f_r small), this additional improvement may be worth the additional complication.

REFERENCES

1. Andrews, G.A., "Airborne Radar Motion Compensation Techniques, Evaluation of TACCAR," NRL Report 7407, Dec. 1971.
2. Skolnik, M.I., ed., "Radar Handbook," New York: McGraw-Hill, 1970.
3. Dickey, F.R., Jr., and Santa, M.M., "Final Report on Anticlutter Techniques," General Electric Company, Heavy Military Electronics Dept., Report No. R65EMH37, Syracuse, N.Y., 1953.
4. Final Engineering Report on Displaced Phase Center Antenna, Vols. 1-3, Contract AF33(600)-24744, General Electric Company, Schenectady, N.Y., 1956-1957.

**APPENDIX A
DERIVATION OF PHASE ADVANCE DUE TO PLATFORM MOTION**

Instead of using Eq. (3) from the text for f'_d , an alternate form results from subtracting Eq. (2) from Eq. (1):

$$\begin{aligned} f'_d &= f_d - \bar{f}_d \\ &= -2 \frac{v_z}{\lambda} (\cos \theta_s - \cos \theta_a) \end{aligned}$$

where

$$v_z = v_P \cos \phi_s .$$

With a constant scan rate $\dot{\theta}$,

$$\theta_a \rightarrow \theta_a + \dot{\theta} t$$

so that

$$f'_d = -2 \frac{v_z}{\lambda} [\cos \theta_s - \cos(\theta_a + \dot{\theta} t)] ,$$

and

$$\begin{aligned} \eta &= \int_0^T 2\pi f'_d dt && \text{(A1)} \\ &= -\frac{4\pi v_z T}{\lambda} \left[\cos \theta_s - \left(\frac{\sin \frac{\dot{\theta} T}{2}}{\frac{\dot{\theta} T}{2}} \right) \cos \left(\theta_a + \frac{\dot{\theta} T}{2} \right) \right] . \end{aligned}$$

The product $\dot{\theta} T$ represents the angular scan of the antenna during the interpulse period T . For many radar applications this is very small. Therefore,

$$\dot{\theta} T \rightarrow 0$$

which implies that η can be approximated by

$$\begin{aligned}\eta' &= -\frac{4\pi v_z T}{\lambda} (\cos\theta_s - \cos\theta_a) \\ &= -\frac{4\pi v_z T}{\lambda} (\cos(\theta_a + \theta) - \cos\theta_a) \\ &= -\frac{4\pi v_z T}{\lambda} (\cos\theta_a (\cos\theta - 1) - \sin\theta_a \sin\theta).\end{aligned}$$

Using Eq. (3)

$$\eta' = 2\pi f'_d T = 2\pi \frac{f'_d}{f_r}.$$

This is the result that would have been obtained by assuming f'_d to be constant with respect to time in Eq. (A1) and integrating immediately.

**APPENDIX B
DERIVATION OF THE TRANSFER FUNCTION OF AN MTI WITH DPCA**

An n -stage MTI with DPCA applied to the first stage is shown in Fig. B1(a). From Eq. (5),

$$\Delta(\theta) = jG(\theta) \tan \frac{\eta}{2}.$$

Therefore, Fig. B1(a) can be redrawn as shown in Fig. B1(b). The transfer function is given by the Fourier transform of the impulse response, i.e., by

$$H_n(\omega) = \int_{-\infty}^{\infty} h_n(t) e^{-j\omega t} dt$$

where $h_n(t)$ is the impulse response of the system.

Considering the first stage first and then the remaining $n-1$ stages,

$$H_n(\omega) = H_1(\omega)H_{n-1}(\omega)$$

as shown in Fig. B1(c). $H_1(\omega)$ is the transfer function of the first stage and $H_{n-1}(\omega)$ is the transfer function of the last $n-1$ stages.

The impulse response of the first stage is

$$h_1(t) = \left(1 - j \tan \frac{\eta}{2}\right) \delta(t) - \left(1 + j \tan \frac{\eta}{2}\right) \delta(t - T).$$

The transfer function of the first stage is

$$\begin{aligned} H_1(\omega) &= \int_{-\infty}^{\infty} h_1(t) e^{-j\omega t} dt \\ &= \left(1 - j \tan \frac{\eta}{2}\right) - \left(1 + j \tan \frac{\eta}{2}\right) e^{-j\omega T}. \end{aligned}$$

Letting $z = e^{j\omega T}$ gives

$$\begin{aligned} H_1(z) &= \left(1 - j \tan \frac{\eta}{2}\right) - \left(1 + j \tan \frac{\eta}{2}\right) \frac{1}{z} \\ &= \left(1 - j \tan \frac{\eta}{2}\right) \left(\frac{z - \frac{1 + j \tan(\eta/2)}{1 - j \tan(\eta/2)}}{z} \right) \end{aligned}$$

But

$$\begin{aligned} \frac{1 + j \tan \frac{\eta}{2}}{1 - j \tan \frac{\eta}{2}} &= \frac{\left(1 + j \tan \frac{\eta}{2}\right)^2}{1 + \tan^2 \frac{\eta}{2}} \\ &= \frac{1 - \tan^2 \frac{\eta}{2} + j \left(2 \tan \frac{\eta}{2}\right)}{1 + \tan^2 \frac{\eta}{2}} \\ &= \frac{\cos^2 \frac{\eta}{2} - \sin^2 \frac{\eta}{2} + j \left(2 \sin \frac{\eta}{2} \cos \frac{\eta}{2}\right)}{\cos^2 \frac{\eta}{2} + \sin^2 \frac{\eta}{2}} \\ &= \cos \eta + j \sin \eta = e^{j\eta}. \end{aligned}$$

Therefore

$$H_1(z) = \left(1 - j \tan \frac{\eta}{2}\right) \left(\frac{z - e^{j\eta}}{z}\right).$$

A similar derivation for the last $n-1$ stages leads to

$$H_{n-1}(z) = \left(\frac{z-1}{z}\right)^{n-1},$$

assuming binomial weights for the last $n-1$ stages. Combining these results gives

$$H_n(z) = \left(1 - j \tan \frac{\eta}{2}\right) \left(\frac{z - e^{j\eta}}{z}\right) \left(\frac{z-1}{z}\right)^{n-1}$$

The above equation shows that the zero of the first stage is rotated by an angle η in the z plane.

Returning to the frequency domain by letting $z = e^{j\omega T}$ leads to

$$H_1(\omega) = \left(1 - j \tan \frac{\eta}{2}\right) e^{-j[(\omega T - \eta - \pi)/2]} \left[2 \sin \left(\frac{\omega T - \eta}{2}\right)\right]$$

and

$$H_{n-1}(\omega) = e^{-j(n-1)[(\omega T - \pi)/2]} \left[2 \sin \frac{\omega T}{2}\right]^{n-1}$$

Therefore an n -stage MTI with DPCA has a transfer function given by

$$H_n(\omega) = j^n \left(1 - j \tan \frac{\eta}{2}\right) e^{-j[(n\omega T - \eta)/2]} \left[2 \sin\left(\frac{\omega T - \eta}{2}\right)\right] \left[2 \sin \frac{\omega T}{2}\right]^{n-1}$$

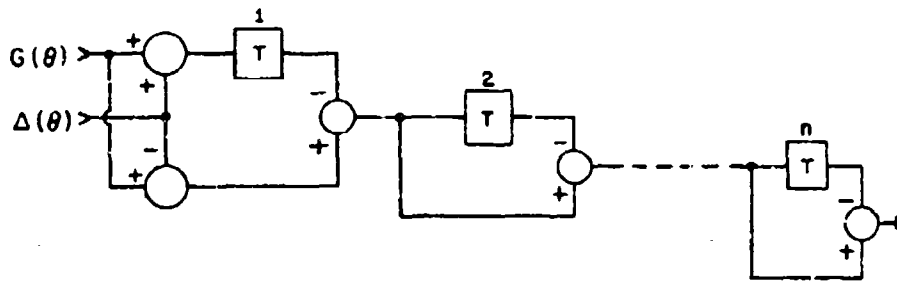
Letting

$$\eta = 2\pi \frac{f'_d}{f_r} \quad \text{and} \quad T = \frac{1}{f_r},$$

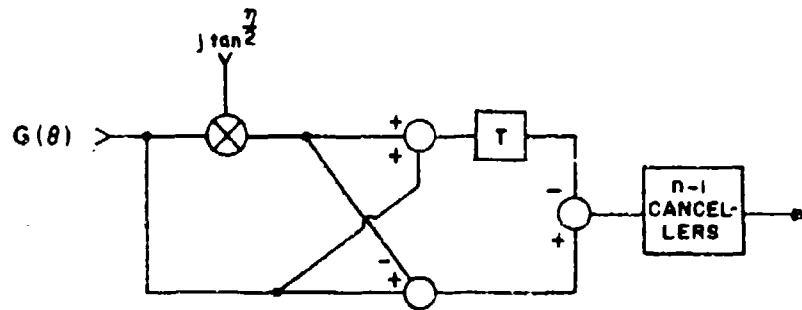
then

$$H_n(f) = j^n \left(1 - j \tan \frac{\eta}{2}\right) e^{-j[\eta n(f/f_r) - (\eta/2)]} \left[2 \sin\left(\pi \frac{f - f'_d}{f_r}\right)\right] \left[2 \sin\left(\pi \frac{f}{f_r}\right)\right]^{n-1}.$$

This equation shows that the zero of the first cancellor is shifted to a frequency f'_d . This corresponds to rotation of the zero in the z plane by an angle η .



(a)



(b)



(c)

Fig. B1—An n -stage MTI with DPCA correction applied to the first stage (a). Replacing $\Delta(\theta)$ by $jG(\theta) \tan(\eta/2)$ allows sketch (a) to be redrawn (b). The transfer function $H_n(\omega)$ is also illustrated (c).

APPENDIX C
DERIVATION OF THE MTI IMPROVEMENT FACTOR WITH DPCA

Assume a Gaussian clutter spectrum given by

$$W(f) = W_0 e^{-1/2(f^2/\sigma_c^2)}$$

The clutter power received at an angle θ with respect to the axis of the antenna pattern has a mean doppler given by Eq. (3) of the text and is amplitude modulated by the antenna power pattern, $G^4(\theta)$. Therefore, this clutter is described by

$$W(f, \theta) = W_0 G^4(\theta) e^{-1/2[(f-f'_d)/\sigma_c]^2} \quad (C1)$$

The total input clutter power from the mainbeam is

$$P_{ic} = \int_{-\theta_0}^{\theta_0} \int_{-\infty}^{\infty} W(f, \theta) df d\theta$$

where θ_0 corresponds to integration over the mainbeam.

Using Eq. (C1) and integrating with respect to frequency yields

$$P_{ic} = W_0 \sqrt{2\pi} \sigma_c \int_{-\theta_0}^{\theta_0} G^4(\theta) d\theta \quad (C2)$$

From App. B the power gain of the n -stage MTI with DPCA is

$$|H_n(f)|^2 = \left(1 + \tan^2 \pi \frac{f'_d}{f_r}\right) \left[2 \sin \left(\pi \frac{f-f'_d}{f_r}\right)\right]^2 \left[2 \sin \left(\pi \frac{f}{f_r}\right)\right]^{2n-2}$$

The output clutter power is given by

$$\begin{aligned} P_{0c} &= \int_{-\theta_0}^{\theta_0} \int_{-\infty}^{\infty} W(f, \theta) |H_n(f)|^2 df d\theta \\ &= W_0 \int_{-\theta_0}^{\theta_0} G^4(\theta) \left(1 + \tan^2 \pi \frac{f'_d}{f_r}\right) H_n(\theta) d\theta \end{aligned} \quad (C3)$$

where

$$H_n(\theta) = \int_{-\infty}^{\infty} \left[2 \sin \left(\pi \frac{f-f_d}{f_r} \right) \right]^2 \left[2 \sin \left(\pi \frac{f}{f_r} \right) \right]^{2n-2} \exp \left[-\frac{1}{2} \left(\frac{f-f_d}{\sigma_c} \right)^2 \right] df.$$

From App. A of Ref. 1, the average target gain \bar{G} is

$$\bar{G} = \frac{2^n}{n!} [1 \cdot 3 \cdot 5 \cdots (2n-1)].$$

The MTI improvement factor, then, is

$$I'_n = \bar{G} \frac{P_{ic}}{P_{0c}} = \frac{2^n [1 \cdot 3 \cdot 5 \cdots (2n-1)] \sqrt{2\pi} \sigma_c \int_{-\theta_0}^{\theta_0} G^4(\theta) d\theta}{n! \int_{-\theta_0}^{\theta_0} G^4(\theta) \left(1 + \tan^2 \pi \frac{f_d}{f_r} \right) H_n(\theta) d\theta}. \quad (C5)$$

Further evaluation of the MTI improvement factor requires that the antenna pattern $G(\theta)$ be specified and $H_n(\theta)$ be derived.

For a Single Canceller ($n=1$)

$$H_1(\theta) = \int_{-\infty}^{\infty} \left[2 \sin \left(\pi \frac{f-f_d}{f_r} \right) \right]^2 \exp \left[-\frac{1}{2} \left(\frac{f-f_d}{\sigma_c} \right)^2 \right] df.$$

For successful MTI action it is necessary that the inequality

$$\sigma_c \ll f_r$$

holds true. Using this fact, and letting

$$f - f_d = x$$

and

$$df = dx$$

gives

$$H_1(\theta) = \left(\frac{2\pi}{f_r} \right)^2 \int_{-\infty}^{\infty} x^2 \exp \left(-\frac{1}{2} \frac{x^2}{\sigma_c} \right) dx.$$

Evaluating this integral* leads to

*Peirce, B.O., "A Short Table of Integrals," Boston: Ginn, 1929; 4th Ed., revised by R.M. Foster, 1956.

$$H_1(\theta) = \sqrt{2\pi} \sigma_c \left(\frac{2\pi\sigma_c}{f_r} \right)^2, \quad (C6)$$

which is not a function of f'_d , and therefore not a function of θ .

Double Canceller ($n = 2$)

For a double canceller

$$H_2(\theta) = \int_{-\infty}^{\infty} \left[2 \sin \left(\pi \frac{f-f'_d}{f_r} \right) \right]^2 \left[2 \sin \left(\pi \frac{f}{f_r} \right) \right]^2 \exp \left[-\frac{1}{2} \left(\frac{f-f'_d}{\sigma_c} \right)^2 \right] df.$$

Again letting $x = f - f'_d$ yields

$$\begin{aligned} H_2(\theta) &= \int_{-\infty}^{\infty} \left[2 \sin \left(\pi \frac{x}{f_r} \right) \right]^2 \left[2 \sin \left(\pi \frac{x+f'_d}{f_r} \right) \right]^2 \exp \left[-\frac{1}{2} \frac{x^2}{\sigma_c^2} \right] dx \\ &= 2^4 \int_{-\infty}^{\infty} \sin^2 \left(\pi \frac{x}{f_r} \right) \left[\sin \left(\pi \frac{f'_d}{f_r} \right) \cos \left(\pi \frac{x}{f_r} \right) + \cos \left(\pi \frac{f'_d}{f_r} \right) \sin \left(\pi \frac{x}{f_r} \right) \right]^2 \\ &\quad \times \exp \left[-\frac{1}{2} \frac{x^2}{\sigma_c^2} \right] dx. \end{aligned}$$

So

$$\begin{aligned} H_2(\theta) &= 2^4 \left[\sin^2 \left(\pi \frac{f'_d}{f_r} \right) \int_{-\infty}^{\infty} \sin^2 \left(\pi \frac{x}{f_r} \right) \cos^2 \left(\pi \frac{x}{f_r} \right) \exp \left(-\frac{1}{2} \frac{x^2}{\sigma_c^2} \right) dx \right. \\ &\quad + \cos^2 \left(\pi \frac{f'_d}{f_r} \right) \int_{-\infty}^{\infty} \sin^4 \left(\pi \frac{x}{f_r} \right) \exp \left(-\frac{1}{2} \frac{x^2}{\sigma_c^2} \right) dx \\ &\quad \left. + 2 \sin \left(\pi \frac{f'_d}{f_r} \right) \cos \left(\pi \frac{f'_d}{f_r} \right) \int_{-\infty}^{\infty} \sin^3 \left(\pi \frac{x}{f_r} \right) \cos \left(\pi \frac{x}{f_r} \right) \exp \left(-\frac{x^2}{2\sigma_c^2} \right) dx \right]. \end{aligned}$$

Since the integrand of the third integral in the above equation is an odd function, therefore the value of that integral is zero. Using the trigonometric identity $\sin 2A = 2 \sin A \cos A$ in the first integral gives

$$\begin{aligned} H_2(\theta) &= \sin^2 \left(\pi \frac{f'_d}{f_r} \right) \int_{-\infty}^{\infty} \left[2 \sin \left(2\pi \frac{x}{f_r} \right) \right]^2 \exp \left(-\frac{x^2}{2\sigma_c^2} \right) dx \\ &\quad + \cos^2 \left(\pi \frac{f'_d}{f_r} \right) \int_{-\infty}^{\infty} \left[2 \sin \left(\pi \frac{x}{f_r} \right) \right]^4 \exp \left(-\frac{x^2}{2\sigma_c^2} \right) dx. \end{aligned}$$

And, as before, letting $\sigma_c \ll f_r$ leads to

$$H_2(\theta) = 4\sqrt{2\pi} \sigma_c \left(\frac{2\pi\sigma_c}{f_r}\right)^2 \sin^2\left(\pi\frac{f_d'}{f_r}\right) + 3\sqrt{2\pi} \sigma_c \left(\frac{2\pi\sigma_c}{f_r}\right)^4 \cos^2\left(\pi\frac{f_d'}{f_r}\right). \quad (C7)$$

Triple Canceller ($n = 3$)

For a triple canceller,

$$H_3(\theta) = \int_{-\infty}^{\infty} \left[2 \sin\left(\pi\frac{f-f_d'}{f_r}\right)\right]^2 \left[2 \sin\left(\pi\frac{f}{f_r}\right)\right]^4 \exp\left[-\frac{1}{2}\left(\frac{f-f_d'}{\sigma_c}\right)^2\right] df.$$

Letting $x = f - f_d'$ yields

$$H_3(\theta) = \int_{-\infty}^{\infty} \left[2 \sin\left(\pi\frac{x}{f_r}\right)\right]^2 \left\{2 \left[\sin\left(\pi\frac{f_d'}{f_r}\right) \cos\left(\pi\frac{x}{f_r}\right) + \cos\left(\pi\frac{f_d'}{f_r}\right) \sin\left(\pi\frac{x}{f_r}\right)\right]\right\}^4 \\ \times \exp\left(-\frac{x^2}{2\sigma_c^2}\right) dx.$$

Expanding this integrand and eliminating all odd powers of $\sin[\pi(x/f_r)]$, whose integral is zero, leads to

$$H_3(\theta) = \sin^4\left(\pi\frac{f_d'}{f_r}\right) \int_{-\infty}^{\infty} 2^6 \cos^4\left(\pi\frac{x}{f_r}\right) \sin^2\left(\pi\frac{x}{f_r}\right) \exp\left(-\frac{x^2}{2\sigma_c^2}\right) dx \\ + 6 \sin^2\left(\pi\frac{f_d'}{f_r}\right) \cos^2\left(\pi\frac{f_d'}{f_r}\right) \int_{-\infty}^{\infty} 2^6 \cos^2\left(\pi\frac{x}{f_r}\right) \sin^4\left(\pi\frac{x}{f_r}\right) \exp\left(-\frac{x^2}{2\sigma_c^2}\right) dx \\ + \cos^4\left(\pi\frac{f_d'}{f_r}\right) \int_{-\infty}^{\infty} 2^6 \sin^6\left(\pi\frac{x}{f_r}\right) \exp\left(-\frac{x^2}{2\sigma_c^2}\right) dx.$$

Letting $\sigma_c \ll f_r$, these integrals can be evaluated as before:

$$H_3(\theta) = 2^4 \left(\frac{2\pi}{f_r}\right)^2 \sin^4\left(\pi\frac{f_d'}{f_r}\right) \int_{-\infty}^{\infty} x^2 \exp\left(-\frac{x^2}{2\sigma_c^2}\right) dx \\ + 6(2^2) \left(\frac{2\pi}{f_r}\right)^4 \sin^2\left(\pi\frac{f_d'}{f_r}\right) \cos^2\left(\pi\frac{f_d'}{f_r}\right) \int_{-\infty}^{\infty} x^4 \exp\left(-\frac{x^2}{2\sigma_c^2}\right) dx \\ + \left(\frac{2\pi}{f_r}\right)^6 \cos^4\left(\pi\frac{f_d'}{f_r}\right) \int_{-\infty}^{\infty} x^6 \exp\left(-\frac{x^2}{2\sigma_c^2}\right) dx.$$

Evaluating these integrals yields

$$\begin{aligned}
 H_3(\theta) = & \sqrt{2\pi} \sigma_c 2^4 \left(\frac{2\pi\sigma_c}{f_r} \right)^2 \sin^4 \left(\pi \frac{f'_d}{f_r} \right) \\
 & + 6(2^2)(3) \sqrt{2\pi} \sigma_c \left(\frac{2\pi\sigma_c}{f_r} \right)^4 \sin^2 \left(\pi \frac{f'_d}{f_r} \right) \cos^2 \left(\pi \frac{f'_d}{f_r} \right) \\
 & + 15 \sqrt{2\pi} \sigma_c \left(\frac{2\pi\sigma_c}{f_r} \right)^6 \cos^4 \left(\pi \frac{f'_d}{f_r} \right). \quad (C8)
 \end{aligned}$$

Using Eqs. (C5)-(C8), the MTI improvement factors for a single, double, and triple canceller with DPCA can be obtained. For a single canceller,

$$\begin{aligned}
 I'_1 &= 2 \left(\frac{f_r}{2\pi\sigma_c} \right)^2 \frac{\int_{-\theta_0}^{\theta_0} G^4(\theta) d\theta}{\int_{-\theta_0}^{\theta_0} \left[1 + \tan^2 \left(\pi \frac{f'_d}{f_r} \right) \right] G^4(\theta) d\theta} \\
 &= I_1 \frac{\int_{-\theta_0}^{\theta_0} G^4(\theta) d\theta}{\int_{-\theta_0}^{\theta_0} \left[1 + \tan^2 \left(\pi \frac{f'_d}{f_r} \right) \right] G^4(\theta) d\theta} \quad (C9)
 \end{aligned}$$

where $I_1 [= 2(f_r/2\pi\sigma_c)^2]$ is the MTI improvement factor for an MTI without platform motion or with perfect motion compensation. Therefore the remaining part of Eq. (C9) can be considered as a loss due to the imperfect compensation of DPCA. For a double canceller,

$$\begin{aligned}
 I'_2 &= 2 \left(\frac{f_r}{2\pi\sigma_c} \right)^4 \frac{3 \int_{-\theta_0}^{\theta_0} G^4(\theta) d\theta}{\int_{-\theta_0}^{\theta_0} G^4(\theta) \left[1 + \tan^2 \left(\pi \frac{f'_d}{f_r} \right) \right] \left[3 \cos^2 \left(\pi \frac{f'_d}{f_r} \right) + 4 \left(\frac{f_r}{2\pi\sigma_c} \right)^2 \sin^2 \left(\pi \frac{f'_d}{f_r} \right) \right] d\theta} \\
 &= I_2 \frac{\int_{-\theta_0}^{\theta_0} G^4(\theta) d\theta}{\int_{-\theta_0}^{\theta_0} G^4(\theta) \left[1 + \tan^2 \left(\pi \frac{f'_d}{f_r} \right) \right] \left[\cos^2 \left(\pi \frac{f'_d}{f_r} \right) + \frac{2}{3} I_1 \sin^2 \left(\pi \frac{f'_d}{f_r} \right) \right] d\theta}
 \end{aligned}$$

where

$$I_2 = 2 \left(\frac{f_r}{2\pi\sigma_c} \right)^4$$

and

$$I_1 = 2 \left(\frac{f_r}{2\pi\sigma_c} \right)^2$$

Using the trigonometric identity

$$1 + \tan^2 A = 1 + \frac{\sin^2 A}{\cos^2 A} = \frac{\cos^2 A + \sin^2 A}{\cos^2 A} = \frac{1}{\cos^2 A}$$

yields

$$I'_2 = I_2 \frac{\int_{-\theta_0}^{\theta_0} G^4(\theta) d\theta}{\int_{-\theta_0}^{\theta_0} G^4(\theta) \left[1 + \frac{2}{3} I_1 \tan^2 \left(\pi \frac{f'_d}{f_r} \right) \right] d\theta} \quad (C10)$$

As before, a loss term is identified in Eq. (C10). Finally, for a triple canceller,

$$I'_3 = \frac{4}{3} \left(\frac{f_r}{2\pi\sigma_c} \right)^6 \frac{15 \int_{-\theta_0}^{\theta_0} G^4(\theta) d\theta}{\left(\int_{-\theta_0}^{\theta_0} G^4(\theta) \left[1 + \tan^2 \left(\pi \frac{f'_d}{f_r} \right) \right] \left[15 \cos^4 \left(\pi \frac{f'_d}{f_r} \right) + 72 \left(\frac{f_r}{2\pi\sigma_c} \right)^2 \sin^2 \left(\pi \frac{f'_d}{f_r} \right) \cos^2 \left(\pi \frac{f'_d}{f_r} \right) + 16 \left(\frac{f_r}{2\pi\sigma_c} \right)^4 \sin^4 \left(\pi \frac{f'_d}{f_r} \right) \right] d\theta \right)} \quad (C11)$$

$$= I_3 \frac{\int_{-\theta_0}^{\theta_0} G^4(\theta) d\theta}{\int_{-\theta_0}^{\theta_0} G^4(\theta) \left[\cos^2 \left(\pi \frac{f'_d}{f_r} \right) + \frac{36}{15} I_1 \sin^2 \left(\pi \frac{f'_d}{f_r} \right) + \frac{8}{15} I_2 \sin^2 \left(\pi \frac{f'_d}{f_r} \right) \tan^2 \left(\pi \frac{f'_d}{f_r} \right) \right] d\theta}$$

where

$$I_3 = \frac{4}{3} \left(\frac{f_r}{2\pi\sigma_c} \right)^6$$

$$I_2 = 2 \left(\frac{f_r}{2\pi\sigma_c} \right)^4$$

and

$$I_1 = 2 \left(\frac{f_r}{2\pi\sigma_c} \right)^2$$

Therefore, the MTI improvement factor with DPCA is given by Eq. (C9) for a single canceller, by Eq. (C10) for a double canceller, by Eq. (C11) for a triple canceller, and can be calculated from Eq. (C5) for an n -stage canceller.

APPENDIX D
EVALUATION OF DPCA WITH A $\sin x/x$ ANTENNA PATTERN

For a $(\sin x)/x$ antenna pattern,

$$G^4(\theta) = \left[\frac{\sin\left(\pi \frac{a}{\lambda} \sin\theta\right)}{\pi \frac{a}{\lambda} \sin\theta} \right]^4$$

where a is the aperture length of the antenna and λ is the transmitted wavelength.

Integrating over the main lobe implies that

$$-\pi \leq \pi \frac{a}{\lambda} \sin\theta \leq \pi.$$

For a single canceller with DPCA, Eq. (C9) can be rewritten as

$$I'_1 = I_1 \frac{G_0}{G_0 + G_1} \quad (D1)$$

where

$$G_0 \equiv \int_{-\theta_0}^{\theta_0} G^4(\theta) d\theta \quad (D2)$$

and

$$G_1 \equiv \int_{-\theta_0}^{\theta_0} G^4(\theta) \tan^2\left(\pi \frac{f_d}{f_r}\right) d\theta. \quad (D3)$$

For a double canceller, Eq. (C10) can be rewritten as

$$I'_2 = I_2 \frac{G_0}{G_0 + \frac{2}{3} I_1 G_1} \quad (D4)$$

For a triple canceller, Eq. (C11) can be rewritten as

$$I'_3 = I_3 \frac{G_0}{G_2 + \frac{36}{15} I_1 G_3 + \frac{8}{15} I_2 G_4} \quad (D5)$$

where

$$G_2 \equiv \int_{-\theta_0}^{\theta_0} G^4(\theta) \cos^2\left(\pi \frac{f'_d}{f_r}\right) d\theta \quad (D6)$$

$$G_3 \equiv \int_{-\theta_0}^{\theta_0} G^4(\theta) \sin^2\left(\pi \frac{f'_d}{f_r}\right) d\theta, \quad (D7)$$

and

$$G_4 \equiv \int_{-\theta_0}^{\theta_0} G^4(\theta) \sin^2\left(\pi \frac{f'_d}{f_r}\right) \tan^2\left(\pi \frac{f'_d}{f_r}\right) d\theta. \quad (D8)$$

The problem is reduced to the evaluation of G_0 , G_1 , G_2 , G_3 , and G_4 . Letting

$$x = \pi \frac{a}{\lambda} \sin\theta$$

implies that $\sin\theta = (\lambda/\pi a)x$. Thus

$$\cos\theta \equiv (1 - \sin^2\theta)^{1/2} = \frac{\lambda}{\pi a} \left[\left(\frac{\pi a}{\lambda} \right)^2 - x^2 \right]^{1/2},$$

and for $a/\lambda \gg 1$

$$\begin{aligned} dx &= \frac{\pi a}{\lambda} \cos\theta d\theta = \left[\left(\frac{\pi a}{\lambda} \right)^2 - x^2 \right]^{1/2} d\theta \\ &\approx \frac{\pi a}{\lambda} d\theta \end{aligned}$$

and

$$-\pi \leq x \leq \pi.$$

Using the above relationships yields

$$\begin{aligned} G_0 &= \int_{-\pi}^{\pi} \left[\left(\frac{\pi a}{\lambda} \right)^2 - x^2 \right]^{-1/2} \left(\frac{\sin x}{x} \right)^4 dx \\ &\approx \frac{\lambda}{\pi a} \int_{-\pi}^{\pi} \left(\frac{\sin x}{x} \right)^4 dx \end{aligned}$$

and for $f'_d \approx -2(v_y/\lambda) \sin\theta = -2(v_y/\pi a)x$ and $T = 1/f_r$,

$$G_1 = \int_{-\pi}^{\pi} \left[\left(\frac{\pi a}{\lambda} \right)^2 - x^2 \right]^{-1/2} \tan^2 \left(2 \frac{v_y T}{a} x \right) \left(\frac{\sin x}{x} \right)^4 dx$$

$$\approx \frac{\lambda}{\pi a} \int_{-\pi}^{\pi} \tan^2(Cx) \left(\frac{\sin x}{x} \right)^4 dx$$

where $C = 2v_y T/a$. In the same way,

$$G_2 \approx \frac{\lambda}{\pi a} \int_{-\pi}^{\pi} \cos^2(Cx) \left(\frac{\sin x}{x} \right)^4 dx,$$

$$G_3 \approx \frac{\lambda}{\pi a} \int_{-\pi}^{\pi} \sin^2(Cx) \left(\frac{\sin x}{x} \right)^4 dx,$$

and

$$G_4 \approx \frac{\lambda}{\pi a} \int_{-\pi}^{\pi} \sin^2(Cx) \tan^2(Cx) \left(\frac{\sin x}{x} \right)^4 dx.$$

Using these results, Eqs. (D1), (D4), and (D5) can be rewritten as

$$I'_1 = I_1 \frac{G'_0}{G'_0 + G'_1},$$

$$I'_2 = I_2 \frac{G'_0}{G'_0 + \frac{2}{3} I_1 G'_1}, \quad (\text{D10})$$

and

$$I'_3 = I_3 \frac{G'_0}{G'_2 + \frac{36}{15} I_1 G'_3 + \frac{8}{15} I_2 G'_4}, \quad (\text{D11})$$

where

$$G'_0 \equiv \int_{-\pi}^{\pi} \left(\frac{\sin x}{x} \right)^4 dx, \quad (\text{D12})$$

$$G'_1 \equiv \int_{-\pi}^{\pi} \left(\frac{\sin x}{x} \right)^4 \tan^2(Cx) dx. \quad (\text{D13})$$

$$G'_2 \equiv \int_{-\pi}^{\pi} \left(\frac{\sin x}{x}\right)^4 \cos^2(Cx) dx, \quad (D14)$$

$$G'_3 \equiv \int_{-\pi}^{\pi} \left(\frac{\sin x}{x}\right)^4 \sin^2(Cx) dx, \quad (D15)$$

and

$$G'_4 \equiv \int_{-\pi}^{\pi} \left(\frac{\sin x}{x}\right)^4 \sin^2(Cx) \tan^2(Cx) dx \quad (D16)$$

with $C = 2v_y T/a$.

Equations (D12) through (D16) are in a form that can be solved on a computer by any standard integration routine. The evaluation of these integrals is given in Table D1. Equations (D9)-(D11) are plotted in Figs. D1-D3 using Table D1.

Table D1
Calculated Values of the Integrals G'_i Used in Evaluating MFI Improvement Factors
(with DPCA), as a Function of the Motion Parameter x

Integral	Calculated Values for		
	$x = 0.001$	$x = 0.01$	$x = 0.1$
G'_0	1.04	1.04	1.04
G'_1	2.6883×10^{-6}	2.6895×10^{-4}	2.8221×10^{-2}
G'_2	1.04	1.04	1.02
G'_3	2.68828×10^{-6}	2.68766×10^{-4}	2.62634×10^{-2}
G'_4	1.88496×10^{-11}	1.88563×10^{-7}	1.9579×10^{-3}

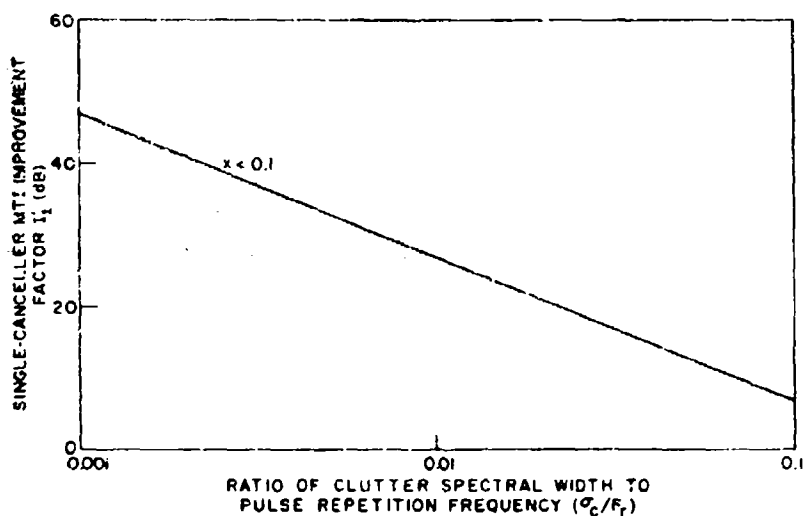


Fig. D1—Effect of platform motion on the single-canceller ($n = 1$) MTI improvement factor I_1' with DPCA. x is the fraction of the antenna aperture that the antenna is displaced per interpulse period. (See Fig. 2.)

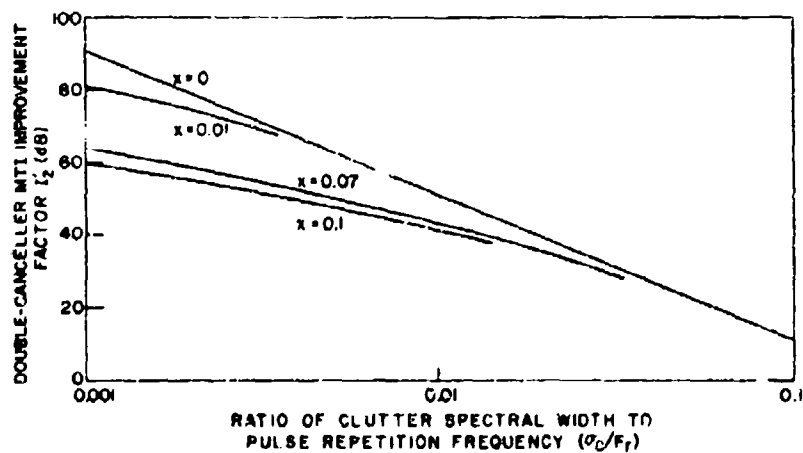


Fig. D2—Effect of platform motion on the double-canceller ($n = 2$) MTI improvement factor I_2' with DPCA. x is the fraction of the antenna aperture that the antenna is displaced per interpulse period. (See Figs. 3 and 7.)

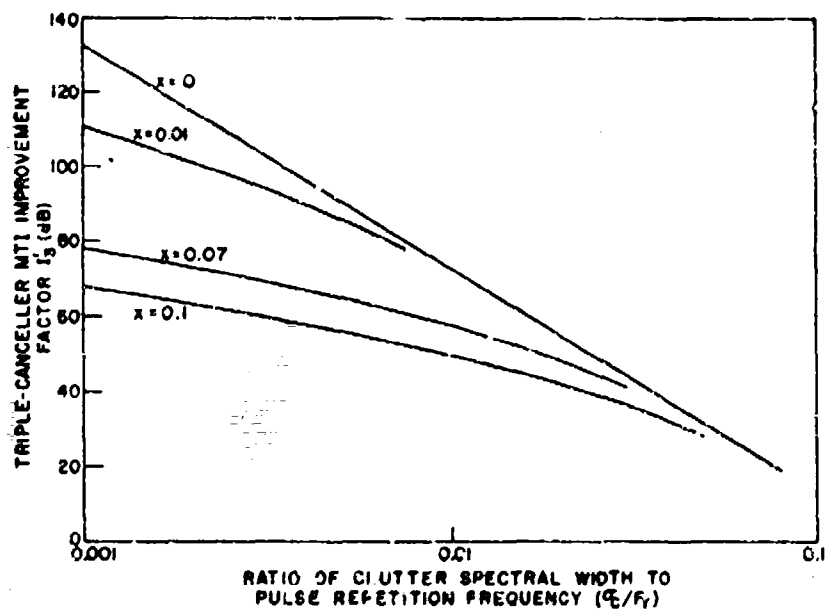


Fig. D8--Effect of platform motion on the triple-canceller ($n = 3$) MTI improvement factor I_3^2 with DPCA. x is the fraction of the antenna aperture that the antenna is displaced per interpulse period. (See Figs. 4 and 8.)

Security Classification

DOCUMENT CONTROL DATA - R & D

(Security classification of title, body of abstract and indexing annotation must be entered when the overall report is classified)

1. ORIGINATING ACTIVITY (Corporate author) Naval Research Laboratory Washington, D.C. 20390		2a. REPORT SECURITY CLASSIFICATION UNCLASSIFIED	
		2b. GROUP	
3. REPORT TITLE Airborne Radar Motion Compensation Techniques--Evaluation of DPCA			
4. DESCRIPTIVE NOTES (Type of report and inclusion dates) Interim report on the problem.			
5. AUTHOR(S) (First name, middle initial, last name) G. A. Andrews			
6. REPORT DATE July 20, 1972		7a. TOTAL NO. OF PAGES 30	7b. NO. OF REFS 5
8a. CONTRACT OR GRANT NO. NRL Problem R02-29		8b. ORIGINATOR'S REPORT NUMBER(S) NRL Report 7426	
8c. PROJECT NO. A360-5333/652B/2F00-141-601		8d. OTHER REPORT NO(S) (Any other numbers that may be assigned this report)	
9. DISTRIBUTION STATEMENT Distribution limited to U.S. Government Agencies only; test and evaluation; July 1972. Other requests for this document must be referred to the Director, Naval Research Laboratory, Washington, D.C. 20390.			
11. SUPPLEMENTARY NOTES		12. SPONSORING MILITARY ACTIVITY Dept. of the Navy (Naval Air Systems Command) Washington, D.C. 20360	
13. ABSTRACT <p>Coherent signal processing in an airborne radar is highly dependent upon methods used to compensate for platform (e.g., airplane) motion. Platform motion causes returns to have doppler shifts which vary with the angle between the velocity vector of the platform and that of the target or scatterer. Because of the finite antenna beamwidth and the finite transmitted pulse length, radar returns from many scatterers are received simultaneously from different angles. Therefore, these returns combine to give a spectrum of doppler frequencies which must be corrected.</p> <p>Displaced Phase Center Antenna (DPCA) is a technique which compensates for the component of motion which is perpendicular to the axis of the beam. This report evaluates DPCA in terms of its improvement to airborne moving target indicator (MTI) performance. It is shown that MTI performance is improved significantly with DPCA. However, since DPCA does not completely compensate for this motion, MTI performance can be limited by this technique under certain conditions.</p>			

DD FORM 1473

(PAGE 1)

3/N 0101-507-6001

27

Security Classification

Security Classification

14 KEY WORDS	LINK A		LINK B		LINK C	
	ROLE	WT	ROLE	WT	ROLE	WT
Airborne						
Radar						
Platform motion						
Compensation						
AMTI						
Airborne moving target indicator						
DPCA						
Displaced phase center antenna						

THIS REPORT HAS BEEN DELIMITED
AND CLEARED FOR PUBLIC RELEASE
UNDER DOD DIRECTIVE 5200.20 AND
NO RESTRICTIONS ARE IMPOSED UPON
ITS USE AND DISCLOSURE.

DISTRIBUTION STATEMENT A

APPROVED FOR PUBLIC RELEASE;
DISTRIBUTION UNLIMITED.